

# Shielding Capabilities of $B_2O_3$ -CdO-ZnO- $K_2O$ - $MoO_3$ Glasses against Gamma Radiation

*R. Umamaheswara Singh<sup>1\*</sup>, K. Chandra Sekhar<sup>2</sup>, Siddoju Rajesham<sup>3</sup>, Chandrasekhar Maalegoundla<sup>4</sup>, Md. Shareefuddin<sup>5</sup>*

<sup>1</sup>Department of Physics, Hyderabad Institute of Technology and Management, Hyderabad, Telangana, 501401, India.

<sup>2</sup>Department of Physics, University College of Science Saifabad, Osmania University, Hyderabad, Telangana, 500004, India.

<sup>3</sup>Geethanjali College of Engineering and Technology, Cheeryal (V), Keesara (M), Medchal-Malkajgiri Dist, Telangana, India.

<sup>4</sup>Matrusri Engineering College, Saidabad, Hyderabad, Telangana, India.

<sup>5</sup>Department of Physics, Osmania University, Hyderabad, Telangana, 500007, India.

**Abstract.** Protective materials are becoming growing in significance in both industrial and daily applications, which has led to an increase in the significance of them in research.  $MoO_3$ , CdO are such high density chemicals which were used to prepare the present glasses with composition  $60B_2O_3$ - $20CdO$ - $10ZnO$ - $(10-x)K_2O$ - $xMoO_3$  where  $x = 0, 0.5, 1, 1.5$  &  $2$ . To determine the sample's amorphous phase, the produced samples were first exposed to the XRD. The spectra's missing distinct peaks demonstrated the materials' amorphous phase. Since greater density offers more protection against radiation penetration, density is essential in radiation-resistant glasses. The concept of Archimedes is used to analyse the glasses' density, and the variance is attributed to the transition of  $BO_3$  and  $BO_4$  units. Shielding properties like MAC and LAC are assessed using Phys-x/PSD software. The PE, CE, and PP in various energy areas are used to describe these factors.

## 1 Introduction

Ionizing radiation-based diagnostic and therapeutic treatments are expected to grow in importance in medicine. When exposed to living beings, ionizing radiation causes chromosomal abnormalities and cancer. Cell damage is proportional to radiation exposure and organ sensitivity. Ionizing radiation can harm workers, patients, and the public, thus safeguards must be taken. The current literature study shows that glassy materials also protect against damaging radiation [1-8]. Borate glasses are the most efficient glass formers and can manufacture glass on their own without any assistance. In addition, they may be coupled with a wide range of additional substances to generate an extensive range of glasses. Even when subjected to slow rates of condensation, glasses formed of  $B_2O_3$  will

---

\* Corresponding author: [rajaputrauma@gmail.com](mailto:rajaputrauma@gmail.com)

not change into a crystalline state. Incorporation of metal oxides into borate glasses gives rise to an enhancement in both the physical and optical qualities of the material [9-11]. The severity of the enhancement is determined by the type and quantity of modifiers that are absorbed into the material. This is made possible by the generation of non-bridging oxygen species in the glass network.

Because the glasses that have been combined with  $B_2O_3$  and  $K_2O$  have an effective atomic number ( $Z_{\text{eff}} = 7.42$ ) that is extremely near to that of human tissue, they are perfect for use in radiation dosimeters that are used in the medical and environmental fields [20-21]. For the purpose of providing protection against gamma rays and other forms of ionizing radiation, they are available as convenient and transparent replacements to concrete. Cadmium oxide (CdO) includes a broad band gap, minimal resistivity, and an increased density, all of which are noteworthy characteristics in terms of its physical and optical properties. Because of its one-of-a-kind characteristics, cadmium oxide (CdO) is suited for a wide variety of purposes, such as materials that shield radiation, photo diodes, transparent electrodes, and many more related uses.[12-17] When ZnO is introduced into borate glasses, it optimizes a variety of optical qualities and, contingent upon the quantity added, it may perform two distinct purposes in the structure of the glass, acting as both a modifier and a formed material[18-19]. The incorporation of zinc oxide into cadmium borate glasses has the potential to significantly enhance the optical parameters such as and gap, refractive index, absorption coefficient, optical basicity. Hence the authors considered the chemicals,  $B_2O_3$ ,  $K_2O$ , CdO, ZnO and  $MoO_3$  for the preparation of glass samples to be investigated with composition  $60B_2O_3-20CdO-10ZnO-(10-x)K_2O-xMoO_3$  where  $x = 0, 0.5, 1, 1.5 \& 2$ . The present paper explains the effect of  $MoO_3$  on the prepared glasses particularly about optical and shielding features.

## 2 Experimental

### 2.1 Sample preparation

The melt quenching method was used to synthesis the glasses that were going to be examined. The compositional formula for these glasses was  $60B_2O_3-20CdO-10ZnO-(10-x)K_2O-xMoO_3$ , where  $x = 0, 0.5, 1, 1.5$ , and 2mol%. From the beginning, the very pure chemicals  $H_3BO_3$ , CdO, ZnO,  $K_2CO_3$ , and  $MoO_3$  were taken into consideration. These chemicals were then weighed according to their molecular weight, carefully mixed in a mortar and grinder. The combination is retained in a crucible and heated in a furnace that is kept on a temperature of one thousand degrees Celsius for one hour. While this was going on, the molten mixes were being swirled in order to achieve homogeneity in the mixture. After that, the molten liquid is put onto a plate made of stainless steel, and then it is instantly pressed in place with another plate made of steel to create the glass samples. In addition, the previously created glasses were annealed for a period of twelve hours in a different furnace that was kept at a temperature of 300 degrees Celsius.

### 2.2 Characterization

An X-ray diffraction (XRD) study is executed on the created glass samples after they have been annealed in order to verify that the samples are amorphous. Philips XPert Pro X-Ray diffractometer was used to record XRD spectra in the  $2\theta$  range of 10 to 80 degrees. After some time has passed, the density of the samples is determined by applying the well-known Archimedes principle. A total of three pieces were selected from each sample, and the density values of each piece of glass were measured. The results were then averaged to

determine the density of each sample, which allowed for the determination of precise density values. Glass samples that had been polished were utilized for the purpose of recording optical absorption spectra in order to get the optical properties. For the purpose of recording absorption plot in the region of 100 nm to 1000 nm, a JASCO UV-Visible spectrometer is utilized. The Phy/PSD online software was utilized in order to conduct an evaluation of the radiation shielding characteristics of the fabricated glasses.

### 3 Results and discussion

#### 3.1 XRD Studies

XRD is a valuable tool for advancing studies related to the glass sector, as it facilitates the understanding of the core characteristics of glasses and the development of new materials. XRD can discover and describe crystalline states or particles contained within bulk glass that may induce faults or modify the glass's characteristics. XRD analyses, particularly high-energy XRD, can reveal the short- and medium-range atomic configurations in glass-making liquids and glasses that affect their attributes such as viscosity and crystal nucleation. The X-ray diffraction spectra of each glass system were studied; the absence of clear, sharp peaks demonstrated that the glasses were amorphous. The X-ray diffraction designs of the current BCZKM glasses are depicted in Figure 1. The XRD analysis revealed no distinct peaks in the spectra, leading to the conclusion that the BCZKM glasses are amorphous.

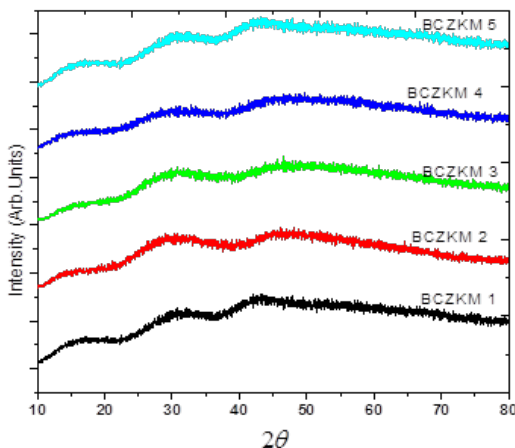


**Fig. 1.** XRD spectra of BCZKM glasses

#### 3.2 Density and molar volume

The density of glass affects its ability to withstand stress and collisions, consequently preserving its underlying structure. Density is a crucial element in trade and production environments, as it affects the effectiveness and utility of glass for numerous uses. Glass samples are assessed by density evaluations, and it is unlikely that two samples from the identical source emerged from the same region if their densities differ markedly. In samples with numerous shards, density readings can function as a screening method to discern different glass sources present.

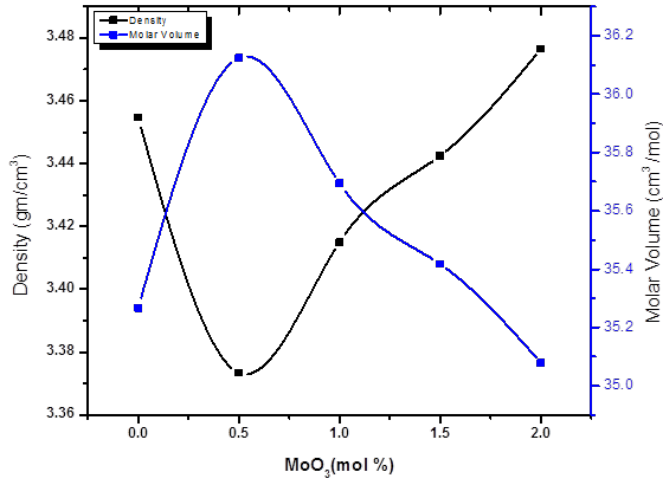


**Fig. 2.** Density and molar volume

A presentation of the obtained density readings for the BCZKM glasses can be found in Table 1. While moving from BCZKN-1 to BCZKM-2, the density value drops as a result of the incorporation of MoO<sub>3</sub>. In addition, the density value noticeably increases from BCZKM-2 to BCZKM-5 when the amount of MoO<sub>3</sub> increases further. According to the density statistics, the glass sample densities increase from 3.3735 to 3.4765 g/cc when MoO<sub>3</sub> grows at the expense of K<sub>2</sub>O. This occurs as the glass sample density incérasses. The translation of BO<sub>3</sub> units into BO<sub>4</sub> units has resulted in a rise in the density. The disparity in density and molar volume occurs in BCZKM glasses in respect to MoO<sub>3</sub> is depicted in Figure 2. When compared to the density values, the molar volume displays a trend that is strikingly different from the density values.

**Table 1:** Physical & Optical Parameters

Physical & Optical parameters	Sample code				
	BCZKM 1	BCZKM 2	BCZKM 3	BCZKM 4	BCZKM 5
Average Molar Weight	121.8370	121.8657	121.8943	121.9230	121.9516
Density ( $\rho$ ) gm/cc	3.4547	3.3735	3.415	3.4425	3.4765
Molar Volume ( $V_m$ ) cc/mol	35.2670	36.1244	35.6938	35.4170	35.0788
Optical Band Gap ( $E_{opt}$ ) eV	3.036	3.006	2.988	2.952	2.919
Refractive Index (n)	2.3874	2.3955	2.4003	2.4101	2.4192
Di Electric Constant ( $\epsilon$ )	5.6999	5.7382	5.7615	5.8087	5.8527
Molar Refractivity ( $R_m$ ) cm <sup>-3</sup>	2.3874	2.3955	2.4003	2.4101	2.4192
Electric Polarizability ( $\sigma_m$ ) 10 <sup>-24</sup> cm <sup>-3</sup>	8.53	8.76	8.67	8.64	8.59
Urbach Energy( $\Delta E$ ) eV	0.6104	0.6123	0.6135	0.6158	0.6180

### 3.3 Radiation Shielding Features

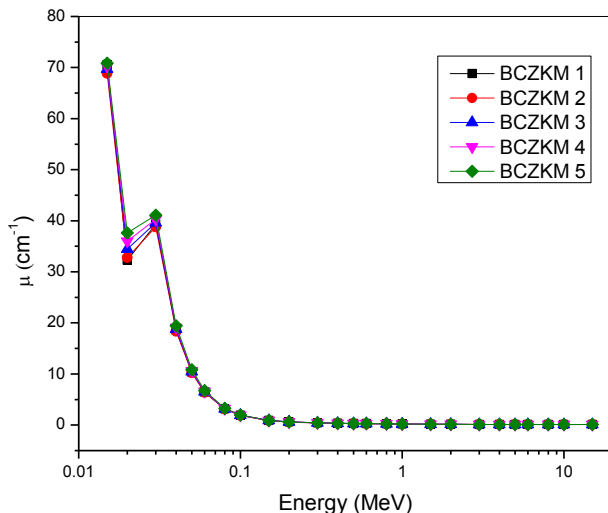


**Fig. 3.** Variation of LAC with the photon energy for prepared BCZKM glass samples

Figure 3 illustrates the LAC of BCZKM glasses concerning the energy of the incident gamma rays. The maximum LAC values occur at lower gamma photon energy because of the strong influence of photoelectric association. The linear attenuation coefficient of Molybdenum-doped lithium borate cadmium zinc glasses diminishes swiftly through rise incoming energy, thru a minor rise at around 0.0200 MeV attributed to the absorption K-edges of Molybdenum. The identified peak is directly correlated to the Molybdenum oxide concentration in the analyzed samples. Within the energy spectrum of 0.1 to 4 MeV, characterized by predominant Compton scattering, the linear attenuation coefficient (LAC) exhibited a considerable decline with increasing gamma photon energies. Above several MeV, the linear attenuation coefficient of BCZKM glasses increases gradually with the incident gamma energy due to the dominance of pair production interactions. For BCZKM 5 with a Molybdenum oxide concentration of 2 mol %, the LAC attains peak values within the range of 0.0945 to 70.87 cm<sup>-1</sup>. At low energies ranging from 0.01 to 0.1 MeV the LAC is increases significantly with the addition of molybdenum oxide, attributable to the dominance of photoelectric interactions which are proportional to Z<sup>4-5</sup>. At an intermediate energy range of 0.1 to 4 MeV, where Compton scattering prevails, the linear attenuation coefficient (LAC) exhibits a gradual increase with rising MoO<sub>3</sub> content, as the Compton scattering cross section is directly proportional to atomic number (Z). Above several MeV, when pair production interactions dominate, the LAC marginally rises with higher molybdenum oxide quantity, as the pair production cross section increases in relation to Z<sup>2</sup>.

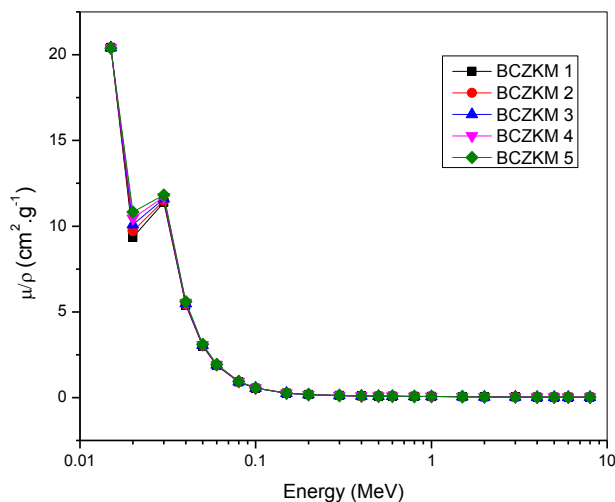


**Fig. 4.** Variation of MAC with the photon energy for prepared BCZKM glassy samples

The estimated mass attenuation coefficient (MAC) of BCZKM glasses, derived from both a simulated linear attenuation coefficient (LAC) and theoretical calculations utilizing Phy-X software. The resulting MAC map is illustrated in Figure 4.

For BCZKM-1, the values vary between 0.02629 to 20.427 cm<sup>2</sup>/g, while the ranges for BCZKM-2, BCZKM-3, BCZKM-4, and BCZKM-5 are 0.02709 to 20.417 cm<sup>2</sup>/g, 0.02712 to 20.407 cm<sup>2</sup>/g, 0.02716 to 20.396 cm<sup>2</sup>/g, and 0.02719 to 20.386 cm<sup>2</sup>/g, respectively. The largest and smallest attenuation coefficients were recorded at the minimum and maximum incident photon energies, respectively, indicating the predominance of analogous coupling modes at each energy level. Higher linearity is documented at the lower end of the energy spectrum due to increased photon interaction. The reduction in attenuation values indicates a decrease in contact likelihood, resulting in enhanced gamma-ray penetration.

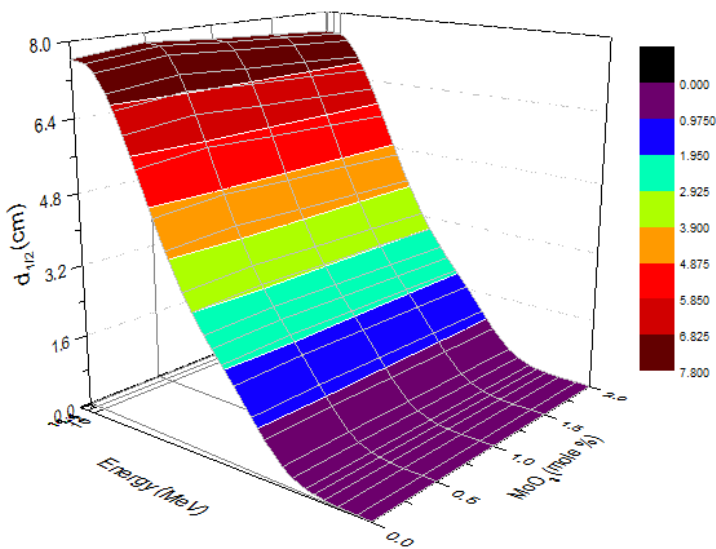


**Fig. 5.** Variation of half value layer ( $d_{1/2}$ ) with respect to MoO<sub>3</sub> concentration (mol. %) and a function of photon energy in the prepared BCZKM glass series

Calculations were made for the present glasses to determine the half-value layer, also known as  $d_{1/2}$ . This is a quantity that is used to estimate the barrier thickness that is required to provide 50% shielding. The variations in  $d_{1/2}$  that occur across different energies and concentrations of MoO<sub>3</sub> are illustrated in Figure 5. The  $d_{1/2}$  value lowers with increasing MoO<sub>3</sub> content and rises with increasing E. For glasses with MoO<sub>3</sub> concentrations of 0, 0.5, 1, 1.5, and 2.0 mol% correspondingly, the minimal  $d_{1/2}$  value was found to be 0.00982, 0.01006, 0.00995, and 0.00987 cm at 15 keV. Finally, the value of 0.00978 cm was found to be the lowest. The half-value layer that corresponds to 15 MeV is 7.632, 7.798, 7.686, 7.608, and 7.517 cm. MoO<sub>3</sub> decreases the amount of thickness of the glass that is required to offer shielding for photons that fall between the spectrum of 15 keV to 15 MeV.

MFP is a technique that measures the average distance that a photon travels before it interacts with another particle. The values that are acquired from this technique demonstrate that the glasses that are being investigated as prospective candidates for radiation shielding exhibit greater effectiveness than commercial glasses. Figure 6 illustrates the MFP results for the chosen glasses across the entire photon energy spectrum, which ranges from 15 keV to 15 MeV. There is a clear indication from the data that the MFP values of the glasses that are being researched go up as the photon energy levels go up.

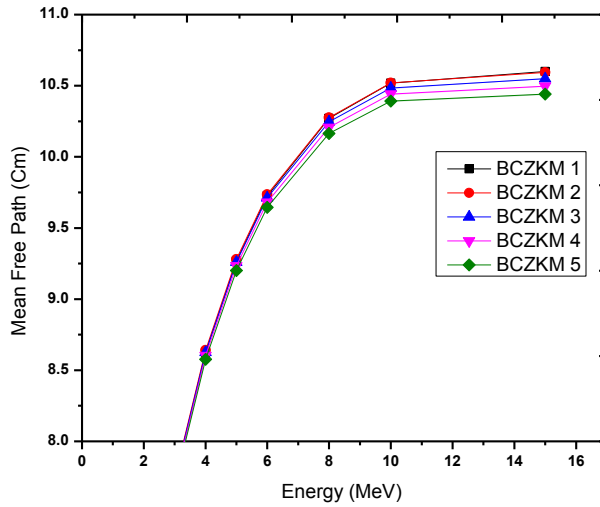


**Fig. 6.** Mean free path (MFP) as a function of photon energy for the glass system BCZKM glasses

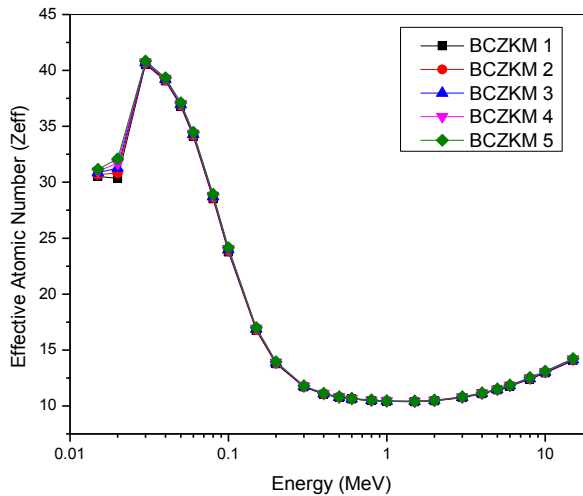


**Fig. 7.** Variations of  $Z_{\text{eff}}$  with the photon energy the prepared BCZKM glass series

Researchers typically make use of the photon interaction variables known as the effective  $Z$  ( $Z_{\text{eff}}$ ) and the effective electron density ( $N_{\text{eff}}$ ) in order to gain an understanding of the ways that the shielding characteristics and dosimetric response of contacting media are affected by the chemical makeup of the media. According to the existing glass system, the anticipated  $Z_{\text{eff}}$  of the BCZKM glasses falls within the following ranges: 10.375 to 40.558, 10.388 to 40.630, 10.402 to 40.700, 10.416 to 40.769, and 10.429 to 40.836, respectively,

for MoO<sub>3</sub> concentrations ranging from 0 to 2 mol%. Figure 7 provides a graphical representation of these distinctions. It is virtually always the case that the attenuation factors and the energy responses of the Z<sub>eff</sub> follow the same pattern. It is common practice to predict a larger Z<sub>eff</sub> from materials that have a greater proportion of elements with greater densities. As a result of MoO<sub>3</sub> having a larger effective Z than K<sub>2</sub>O, the glasses are guaranteed to be able to absorb photons in the BCZKM 1 < BCZKM 2 < BCZKM 3 < BCZKM 4 < BCZKM 5 range.

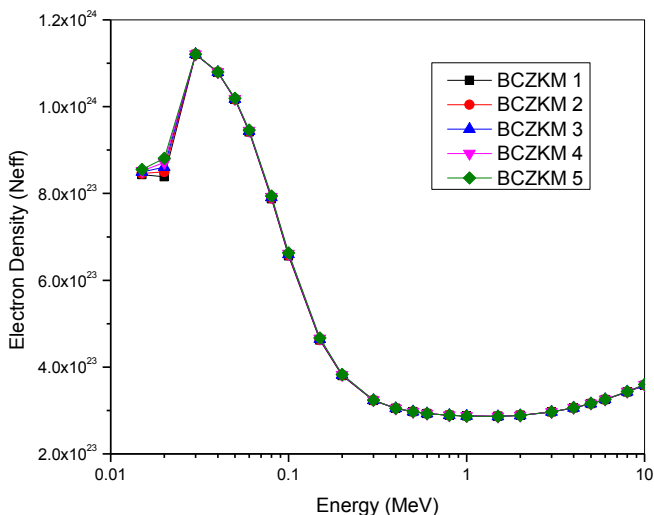


**Fig. 8.** Variations of N<sub>eff</sub> with the photon energy the prepared BCZKM glass series

The shift in the effective atomic number is similarly matched by an alteration in the energy of N<sub>eff</sub>, as can be seen in Figure 8. The value of N<sub>eff</sub> falls between the range of 2.866-11.205, 2.865-11.205, 2.864-11.207, 2.863-11.208, and 2.862-11.208(x1023) electron/g for BCZKM 1, BCZKM 2, BCZKM 3, BCZKM 4, and BCZKM 5, respectively. These values are all within the specified range of the electron density. In contrast to Z<sub>eff</sub>'s arrangement, which is as follows: (N<sub>eff</sub>)BCZKM 5 < (N<sub>eff</sub>)BCZKM 4 < (N<sub>eff</sub>)BCZKM 3 < (N<sub>eff</sub>)BCZKM 2 < (N<sub>eff</sub>)BCZKM 1, these sequences demonstrate the opposite situation. When compared to the remaining segments of the energy spectrum, this pattern is more noticeable for energies that are lower than 0.5 MeV. The pattern that was seen was brought about by the increasing concentration of Mo, which is a heavy atom in compared to K. This is because the number of electrons per unit mass (A/Z) normally decreases as A rises. Furthermore, as compared to CS and PP, the cross-section for PE interaction appears more sensitive to Z. As a consequence, the fluctuations in the N<sub>eff</sub> of the BCZKM glasses are more noticeable in the energy range E < 500 keV, where PE is the dominant phenomenon in the interaction procedures.

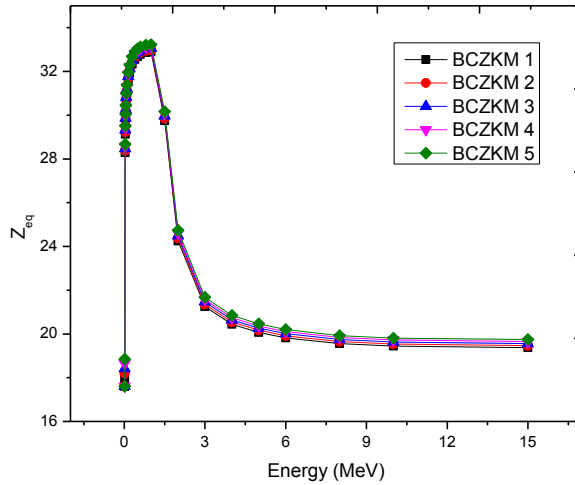


**Fig. 9.** Variations of equivalent atomic numbers of the prepared BCZKM glass series as a function of photon energy

The corresponding atomic number  $Z_{eq}$  is evaluated to assess the photon scattering capability of a safeguard in comparison to that of unadulterated atoms. The calculation might be performed using the Gaussian Process fitting approach. As illustrated in Figure 9, the variable grows fast with energy up to 1 MeV, after which it declines steadily. This augmentation is associated with the rise in incoherent scattering.  $Z_{eq}$  escalates along with the density of material and the quantity of Mo. This augmentation is associated with the rise in disjointed scattering in the interior of the sample.  $Z_{eq}$  escalates along with the density of glass and the quantity of Mo. The maximum  $Z_{eq}$  values of the glasses are 32.89, 32.98, 33.06, 33.14, and 33.23 for MoO<sub>3</sub> contents of 0–2 mol%, respectively.

Figure 10 illustrates the EBF as a function of energy. The EBF augmented with the thickness of the glass owing to numerous scattering. The augmentation of Mo content somewhat enhances the EBF in the prepared samples. According to the investigated criteria, the BCZKM-2 glass demonstrates superior gamma-ray shielding capabilities compared to the other manufactured BCZKM glasses.

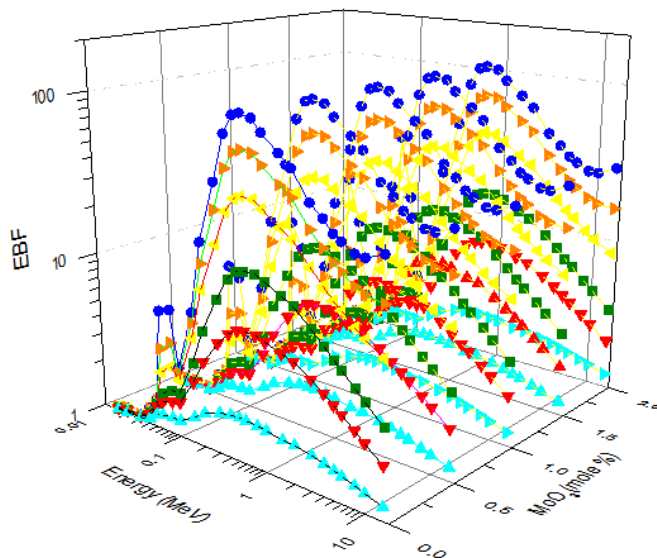


**Fig. 10.** Variation of exposure buildup factor (EBF) with the photon energy for the prepared BCZKM glass series.

## 4 Conclusions

The melt quenching fabrication process was hired to produce the glasses intended for examination. The compositional formula for these glasses is  $60\text{B}_2\text{O}_3\text{-}20\text{CdO-}10\text{ZnO-(}10\text{-}x\text{)K}_2\text{O-}x\text{MoO}_3$ , with  $x$  values of 0, 0.5, 1, 1.5, and 2 mol%. The XRD investigation indicated the absence of identifiable peaks in the spectra, resulting in the conclusion that the BCZKM glasses are amorphous. The density value decreases from BCZKN-1 to BCZKM-2 due to the inclusion of  $\text{MoO}_3$ . The density value significantly rises from BCZKM-2 to BCZKM-5 when the quantity of  $\text{MoO}_3$  climbs further. Minor alterations in the chemical makeup of a glass system may significantly affect its architectural and radiation shielding characteristics. The created glasses exhibit low processing temperatures are transparent, non-toxic, and environmentally friendly. Our engineered glass systems effectively guard against Gamma rays, neutrons, and charged particles.

Samples exhibiting high density at elevated percentage of  $\text{MoO}_3$  could be utilized in radiation protective materials, a sector of significant contemporary relevance. The augmentation of  $\text{MoO}_3$  mole percentage enhanced the material capacity to fascinate gamma rays across a broad spectrum of energy. The augmentation of  $\text{MoO}_3$  amplified photon accumulation in the glasses. Unlike conventional shielding materials, the current glasses may be advantageous because their superior protecting capabilities, without lead composition, and visual clarity.

The manufactured glasses were evaluated for their potential in radiation shielding applications using Phy-X software to determine gamma attenuation parameters, including the LAC, MAC and HVL in optimal transmission geometry. The MACs were subsequently employed to determine the  $Z_{\text{eff}}$  and the glass samples were evaluated for their capacity to

attenuate gamma rays generated from a radioactive source. The MACs, HVLs,  $Z_{\text{effs}}$ , and EBF were computed throughout a continuous energy spectrum, and the build-up factor was assessed for the glass samples at various penetration depths. According to the evaluated parameters, the BCZKM-5 glass demonstrates superior gamma-ray shielding compared to the other manufactured glasses.

## References

1. Vishwanath P. Singh, N. M. Badiger, J. Kaewkhao, *Journal of Non-Crystalline Solids* 404, 167 (2014).
2. M. I. Sayyed, G. Lakshminarayana, M. A. Mahdi, *Chalcogenide Letters* 14(2), 43 (2017)
3. Rachniyom, W.; Chaiphaksa, W.; Limkitjaroenporn, P.; Tuschaoen, S.; Sangwanatee, N.; Kaewkhao, J. Effect of Bi<sub>2</sub>O<sub>3</sub> on radiation shielding properties of glasses from coal fly ash. *Mater. Today Proc.* 2018, 5, 14046–14051.
4. Kavaz, E. An experimental study on gamma ray shielding features of lithium borate glasses doped with dolomite, hematite and goethite minerals. *Radiat. Phys. Chem.* 2019, 160, 112–123.
5. Ashok, K. Gamma ray shielding properties of PbO-Li<sub>2</sub>O-B<sub>2</sub>O<sub>3</sub> glasses. *Radiat. Phys. Chem.* 2017, 136, 50–53.
6. Chanthima, N.; Kaewkhao, J.; Limkitjaroenporn, P.; Tuscharoen, S.; Kothan, S.; Tungjai, M.; Kaewjaeng, S.; Sarachai, S.; Limsuwan, P. Development of BaO–ZnO–B<sub>2</sub>O<sub>3</sub> glasses as a radiation shielding material. *Radiat. Phys. Chem.* 2017, 137, 72–77.
7. Sayyed, M.I.; Al-Hadeethi, Y.; AlShammari, M.M.; Ahmed, M.; Al-Heniti, S.H.; Rammah, Y.S. Physical, optical and gamma radiation shielding competence of newly borotellurite based glasses: TeO<sub>2</sub>–B<sub>2</sub>O<sub>3</sub>–ZnO–Li<sub>2</sub>O<sub>3</sub>–Bi<sub>2</sub>O<sub>3</sub>. *Ceram. Int.* 2021, 47, 611–618.
8. Sayyed, M.I.; Mhareb, M.H.A.; Alajerami, Y.S.M.; Mahmoud, K.A.; Imheidat, M.A.; Alshahri, F.; Alqahtani, M.; Al-Abdullah, T. Optical and radiation shielding features for a new series of borate glass samples. *Optik* 2021, 239, 166790.
9. K. Chandra Sekhar, Abdul Hameed, G. Ramadevudu, M. Narasimha Chary and Md Shareefuddin, Physical and spectroscopic studies on manganese ions in lead halo borate glasses *Mod. Phys. Lett. B* 31 (2017) 1750180.
10. Erkan Ilik, Esra Kavaz, Gokhan Kilic, Shams A.M. Issa, Hesham M.H.Zakaly, H.O.Tekin, A closer-look on Copper(II) oxide reinforced Calcium-Borate glasses: Fabrication and multiple experimental assessment on optical, structural, physical, and experimental neutron/gamma shielding properties, *Ceram. Inter* 48(5) (2022) 6780-6791.
11. A.V. Deepa, P. Murugasen, & S. A Sagadevan, comparative study on lanthanum oxide and holmium oxide doped borate glasses. *Glass Phys Chem* 43 (2017) 233–239.
12. Y.B. Saddeek, H.M.H. Zakaly, K.C. Sekhar, S.A.M. Issa, T. Alharbi, A. Badawi, M. Shareefuddin, Investigations of mechanical and radiation shielding properties of BaTiO<sub>3</sub>modified cadmium alkali borate glass. *Appl. Phys. A*, 128, (2022) 110,
13. H.M.H. Zakaly, S.A.M. Issa, H.O. Tekin, A. Badawi, H.A. Saudi, A.M.A. Henaish, Y.S Rammah. An experimental evaluation of CdO/PbO-B<sub>2</sub>O<sub>3</sub> glasses containing

- neodymium oxide: Structure, electrical conductivity, and gamma-ray resistance. *Mater. Res. Bull.*, 151 (2022)111828,
14. G.A. Alharshan, C. Eke, A.A. Ibraheem,. Hardness, Elastic Properties, and Radiation Shielding Performance of the CdO-P2O5-NiO Glass System. *J. Electron. Mater.* 51 (2022) 5808–5817.
  15. M. Marzouk, H. ElBatal, & W. Eisa, Optical stability of 3d transition metal ions doped-cadmium borate glasses towards  $\gamma$ -rays interaction. *Indian J Phys* 90 (2016) 781–791.
  16. A.S. Abouhaswa, S.A.M. Issa, H.M.H Zakaly, M.M. Hessien, A.A. El-Hamalawy, H. O.Tekin, Y. S. Rammah, Structural, optical, mechanical and simulating the gamma-ray shielding competencies of novel cadmium bismo-borate glasses: The impact of bismuth oxide. *J Mater Sci: Mater Electron* 32 (2021) 24381–24393.
  17. S. Vedavyas, K.C. Sekhar, S. Ahammed, G Ramadevudu, M. Narasimha Chary, Md. Shareefuddin, Physical and structural studies of cadmium lead boro-tellurite glasses doped with Cu<sup>2+</sup> ions. *J Mater Sci: Mater Electron* 32 (2021) 3083–3091.
  18. G Sangeetha. K Chandra Sekhar, A Hameed, G Ramadevudu. M Narasimha Chary, and Md Shareefuddin, Influence of CaO on the structure of zinc sodium tetra borate glasses containing Cu<sup>2+</sup> ions, *J. Non-Cryst. Solids* 563 (2021) 120784.
  19. S.G. Motke, S.P. Yawale, S.S. Yawale, Infrared spectra of zinc doped lead borate glasses, *Bull. Mater. Sci.* 25 (2002) 75–78,.
  20. Sayyed, M.I.; Albarzan, B.;Almuqrin, A.H.; El-Khatib, A.M.;Kumar, A.; Tishkevich, D.I.; Trukhanov, A.V.; Elsafi, M.Experimental and Theoretical Study of Radiation Shielding Features of CaO-K2O-Na2O-P2O5 Glass Systems.*Materials* 2021, 14, 3772.
  21. Abdullaha M.S. Alhuthali, A.Kumar, M.I. Sayyed , Y.Al-hadeethi INVESTIGATIONS OF GAMMA-RAY SHIELDING PROPERTIES OF MoO<sub>3</sub>-modified P2O5-SiO2-K2O-MgO-CaO Glasses, *Digest Journal of Nanomaterials and Biostructures*, Vol. 16, No. 1, January - March 2021, 183 – 189.